Chemical Science

EDGE ARTICLE

View Article Online
View Journal | View Issue

Check for updates

Cite this: *Chem. Sci.*, 2018, **9**, 6580

All publication charges for this article have been paid for by the Royal Society of Chemistry

Received 8th June 2018
Accepted 26th June 2018

DOI: 10.1039/c8sc02536c

rsc.li/chemical-science

Synthesis and reactivity of a nickel(II) thioperoxide complex: demonstration of sulfide-mediated N_2O reduction†

Nathaniel J. Hartmann, Guang Wu and Trevor W. Hayton *

The thiohyponitrite ($[SNNO]^{2-}$) complex, $[K(18\text{-crown-6})][L^{tBu}Ni^{II}(\kappa^2\text{-SNNO})]$ (L^{tBu} = $\{(2,6\text{-}^iPr_2C_6H_3)NC(^tBu)\}_2CH$), extrudes N_2 under mild heating to yield $[K(18\text{-crown-6})][L^{tBu}Ni^{II}(\eta^2\text{-SO})]$ (**1**), along with minor products $[K(18\text{-crown-6})][L^{tBu}Ni^{II}(\eta^2\text{-OSSO})]$ (**2**) and $[K(18\text{-crown-6})][L^{tBu}Ni^{II}(\eta^2\text{-}S_2)]$ (**3**). Subsequent reaction of **1** with carbon monoxide (CO) results in the formation of $[K(18\text{-crown-6})][L^{tBu}Ni^{II}(\eta^2\text{-SCO})]$ (**4**), $[K(18\text{-crown-6})][L^{tBu}Ni^{II}(S,O{:}\kappa^2\text{-}SCO_2)]$ (**5**), $[K(18\text{-crown-6})][L^{tBu}Ni^{II}(\kappa^2\text{-}CO_3)]$ (**6**), carbonyl sulfide (COS) (**7**), and $[K(18\text{-crown-6})][L^{tBu}Ni^{II}(S_2CO)]$ (**8**). To rationalize the formation of these products we propose that **1** first reacts with CO to form $[K(18\text{-crown-6})][L^{tBu}Ni^{II}(S)]$ (**I**) and CO_2, *via* O-atom abstraction. Subsequently, complex **I** reacts with CO or CO_2 to form **4** and **5**, respectively. Similarly, the formation of complex **6** and COS can be rationalized by the reaction of **1** with CO_2 to form a putative Ni(II) monothiopercarbonate, $[K(18\text{-crown-6})][L^{tBu}Ni^{II}(\kappa^2\text{-SOCO}_2)]$ (**11**). The Ni(II) monothiopercarbonate subsequently transfers a S-atom to CO to form COS and $[K(18\text{-crown-6})][L^{tBu}Ni^{II}(\kappa^2\text{-}CO_3)]$ (**6**). Finally, the formation of **8** can be rationalized by the reaction of COS with **I**. Critically, the observation of complexes **4** and **5** in the reaction mixture reveals the stepwise conversion of $[K(18\text{-crown-6})][L^{tBu}Ni^{II}(\kappa^2\text{-SNNO})]$ to **1** and then **I**, which represents the formal reduction of N_2O by CO.

Introduction

Nitrous oxide (N_2O) features a long atmospheric lifetime and large global warming potential (*ca.* 300 times larger than CO_2), making it an important greenhouse gas.[1–4] Anthropogenic sources of N_2O include agriculture, fossil fuel combustion, adipic acid synthesis, and nitric acid production.[1,5] The latter two sources use on-site N_2O mitigation to remove N_2O from the effluent stream, either by decomposition to the elements[6] or reduction to N_2 and H_2O, but neither of these methods is completely effective and some N_2O is still released into the atmosphere.[7]

Given the above considerations, the development of new catalysts for N_2O reduction could help reduce its impact on global temperatures.[1,8] Not surprisingly, a large number of heterogeneous systems have been developed to catalyze this reaction.[9] Of most relevance to the current study are the catalyst systems used for automotive applications, which consist of nanoparticulate Pt and Rh on a ceramic support. This process uses partially oxidized fuel (*i.e.*, CO) to reduce N_2O, forming N_2 and CO_2.[9] Sita and co-workers developed a homogeneous version of this transformation, mediated by the Mo(II) complex, $Cp^*Mo(NCN)(CO)_2$ (NCN = $^iPrNC(Me)N^iPr$).[10] In this process, N_2O oxidizes $Cp^*Mo(NCN)(CO)_2$ to form a Mo(IV) oxo, $Cp^*Mo(NCN)(O)$, which then reacts with CO to form CO_2 and regenerate $Cp^*Mo(NCN)(CO)_2$. However, an N–N bond cleavage reaction, which results in irreversible formation of $Cp^*Mo(NCN)(NCO)(NO)$, was found to be competitive with oxo formation. Similarly, Limberg and co-workers reported the stoichiometric oxidation of a Ni(0) CO complex, $[K]_2[L^{tBu}Ni^0(CO)]_2$, with N_2O to form a carbonate complex, $[K]_6[L^{tBu}Ni^{II}(CO_3)]_6$, and N_2.[11] Subsequent release of carbonate from the metal center was not discussed. The homogeneous hydrogenation of N_2O has also been explored.[12,13] For example, in 2015 Piers and co-workers reported an Ir(III) pincer carbene complex that could hydrogenate N_2O;[14] however, this system was not reported to be catalytic. More recently, Milstein and co-workers reported that the Ru pincer complex, $[(PNP)RuH(CO)(OH)]$ (PNP = $2,6\text{-}[CH_2P^iPr_2]_2(C_5H_3N)$), was an effective catalyst for the hydrogenation of N_2O, achieving a turnover number of *ca.* 400.[15]

Recently, we reported the activation of N_2O by the "masked" terminal nickel sulfide complex, $[K(18\text{-crown-6})][L^{tBu}Ni^{II}(S)]$ (**I**) (L^{tBu} = $\{(2,6\text{-}^iPr_2C_6H_3)NC(^tBu)\}_2CH$), which yielded an unprecedented thiohyponitrite complex, $[K(18\text{-crown-6})][L^{tBu}Ni^{II}(\kappa^2\text{-SNNO})]$ (**II**) (eqn (1)).[16] Given the challenge of activating N_2O,[17] and the novelty of the $[SNNO]^{2-}$ ligand in **II**, we endeavored to

---

Department of Chemistry and Biochemistry, University of California, Santa Barbara, California, 93106 USA. E-mail: hayton@chem.ucsb.edu

† Electronic supplementary information (ESI) available: Experimental and crystallographic details and spectral data. CCDC 1847162–1847167. For ESI and crystallographic data in CIF or other electronic format see DOI: 10.1039/c8sc02536c

explore its reactivity in greater detail. Herein, we describe the first reactivity study of the $[SNNO]^{2-}$ ligand in an effort to uncover new routes to N_2O reduction.

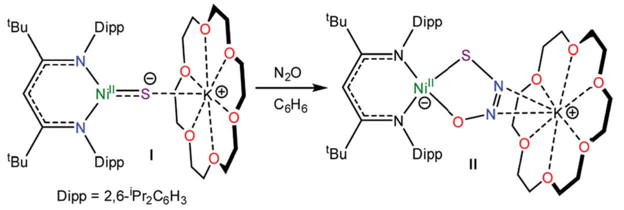

(1)

Results and discussion

Synthesis of an $[\eta^2\text{-SO}]^{2-}$ complex

Gentle heating of a toluene-d_8 solution of $[K(18\text{-crown-6})][L^{tBu}Ni^{II}(\kappa^2\text{-SNNO})]$ (**II**) at 45 °C results in the complete disappearance of **II** over the course of 6 d. A ^1H NMR spectrum of this reaction mixture reveals the presence of a new γ-CH resonance at 5.43 ppm (Fig. S2 and 3†), which we have assigned to the thioperoxide complex, $[K(18\text{-crown-6})][L^{tBu}Ni^{II}(\eta^2\text{-SO})]$ (**1**). A preliminary kinetic analysis suggests that the formation of **1** is first-order with respect to complex **II**, indicating that this transformation is unimolecular (Fig. S25†). Also present in these spectra are two minor γ-CH resonances. The first, observed at 5.53 ppm, has been tentatively assigned to the disulfur dioxide complex, $[K(18\text{-crown-6})][L^{tBu}Ni^{II}(\eta^2\text{-OSSO})]$ (**2**), and the second resonance at 5.47 ppm, has been assigned to the disulfide complex, $[K(18\text{-crown-6})][L^{tBu}Ni^{II}(\eta^2\text{-}S_2)]$ (**3**). Work-up of the reaction mixture affords $[K(18\text{-crown-6})][L^{tBu}Ni^{II}(\eta^2\text{-SO})]$ (**1**) as an orange crystalline solid in 82% yield (eqn (2)). The solid state molecular structure of **1** is shown in Fig. 1. Complex **1** features a rare example of an η²-thioperoxide ($[\eta^2\text{-SO}]^{2-}$) ligand, which is formed *via* N_2 extrusion from the thiohyponitrite fragment. The $[\eta^2\text{-SO}]^{2-}$ ligand in **1** is disordered over two positions in a 97 : 3 ratio, which are related by a C_2 rotation about the Ni–K axis. It possesses an S–O bond length of 1.656(3) Å, consistent with an S–O single bond.[18] For comparison, the S–O distance in free S═O is substantially shorter (1.48108(8) Å), due to its higher bond order.[19] The Ni–S (2.127(1) Å) and Ni–O (1.954(3) Å) distances in **1** are both consistent with single bonds and are comparable with those found in the starting material (**II**), while the Ni–N bond lengths (1.881(4) and 1.900(4) Å) are similar to those observed in other square planar L^RNi^{II} complexes.[16,20]

The ^1H and $^{13}C\{^1H\}$ NMR spectra of **1** are consistent with its formulation as a C_s symmetric, diamagnetic, square planar Ni^{II} complex. The ^1H NMR spectrum of **1** in C_6D_6 features two *tert*-butyl resonances at 1.32 and 1.37 ppm and a single γ-CH resonance at 5.54 ppm. The IR spectrum (KBr pellet) of **1** reveals a strong ν_{SO} mode at 902 cm^{-1}, which is consistent with values reported for other $[\eta^2\text{-SO}]^{2-}$ ligands (883, 873 cm^{-1}).[21,22] Only a handful of structurally-characterized thioperoxide complexes are known,[23–26] including $[(triphos)Rh(\mu\text{-}\eta^2,\eta^1\text{-SO})_2Rh(triphos)][BPh_4]_2$ (triphos = $CH_3C(CH_2PPh_2)_3$), $[\{RhCl(\mu\text{-}\eta^2,\eta^1\text{-SO})(PPh_3)_2\}_2]$, and $Fe_3(\mu_3\text{-SO})(S)(CO)_9$.[21,27,28] The iron example is notable because it can be prepared by O-atom transfer to $Fe_3(S)_2(CO)_9$,[29] a manner of preparation that is similar to that of **1**. Interestingly, Mankad and co-workers suggest that a transient SO complex is formed upon reaction of $[(IPr^*)Cu]_2(\mu\text{-S})$ with N_2O,[30] a transformation that parallels our conversion of **I** to **II** and then **1**.

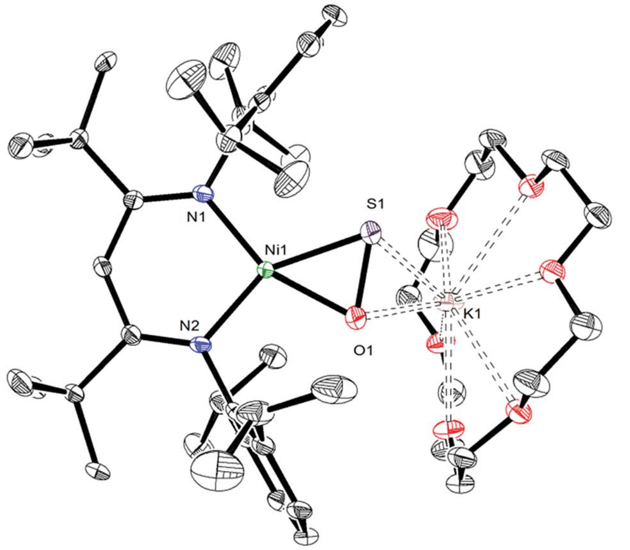

Fig. 1 ORTEP drawing of $[K(18\text{-crown-6})][L^{tBu}Ni^{II}(\eta^2\text{-SO})]\cdot C_7H_8$ ($1\cdot C_7H_8$) shown with 50% thermal ellipsoids. Hydrogen atoms, a C_7H_8 solvate molecule, and one orientation of the disordered $[\eta^2\text{-SO}]^{2-}$ ligand have been omitted for clarity. Selected metrical parameters: S1–O1 1.656(3) Å, Ni1–S1 2.127(1) Å, Ni1–O1 1.954(3) Å, Ni1–N1 1.881(4) Å, Ni1–N2 1.900(4) Å, S1–K1 3.162(2) Å, O1–K1 2.881(3) Å, N1–Ni1–N2 99.2(2)°, N1–Ni1–S1 110.0(1)°, N2–Ni1–O1 103.2(1)°, S1–Ni1–O1 47.65(9)°.

As mentioned above, we also observe formation of $[K(18\text{-crown-6})][L^{tBu}Ni^{II}(\eta^2\text{-OSSO})]$ (**2**), as a minor side product, during the conversion of $[K(18\text{-crown-6})][L^{tBu}Ni^{II}(\kappa^2\text{-SNNO})]$ to **1**. Despite its presence in trace amounts, we have been able to obtain a few single crystals of **2** as orange plates from the reaction mixture. The solid state molecular structure of **2** is shown in Fig. 2. It features the first example of a co-planar $[OSSO]^{2-}$ ligand (OSSO dihedral angle = 2°). The $[\eta^2\text{-OSSO}]^{2-}$ ligand in **2** is bound to the Ni center in an η² fashion, *via* both sulfur atoms, while the O atoms are bound to the $[K(18\text{-crown-6})]^+$ cation in a κ² fashion. Its S–S distance is 2.093(3) Å, while the S–O distances are 1.485(5) and 1.496(7) Å. For comparison, the S–S (2.0245(6) Å) and S–O (1.458(2) Å) distances in free S_2O_2 are shorter than those observed for **2**,[31–33] consistent with the reduced S–S and S–O bond orders anticipated for the $[OSSO]^{2-}$ fragment in the former.[31,34,35] Notably, complex **2** is only the third OSSO complex to be reported and only second to be structurally characterized.[29,36–38]

To account for the presence of **2** in the reaction mixture, we hypothesize that complex **1** undergoes a formal disproportionation, forming **2** and an equivalent of unobserved "$[K(18\text{-crown-6})][L^{tBu}Ni^0]$". However, because of the low yield (typically less than 3% relative to complex **1**, as assessed by ^1H NMR spectroscopy), this transformation must be very inefficient. The low yield has also impeded our ability to fully characterize this complex.

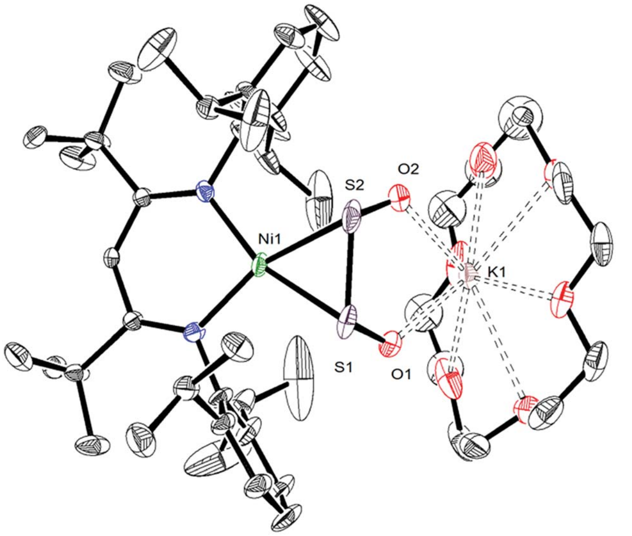

Fig. 2 ORTEP drawing of [K(18-crown-6)][$L^{tBu}Ni^{II}(\eta^2\text{-OSSO})$]·$2C_6H_{14}$ (**2**·$2C_6H_{14}$) shown with 50% thermal ellipsoids. Hydrogen atoms and C_6H_{14} solvate molecules have been omitted for clarity. Selected metrical parameters: S1–S2 2.093(3) Å, S1–O1 1.485(5) Å, S2–O2 1.496(7) Å, Ni1–S1 2.181(2) Å, Ni1–S2 2.173(2) Å, Ni1–N1 1.920(4) Å, Ni1–N2 1.925(4) Å, O1–K1 2.747(4) Å, O2–K1 2.777(6) Å, N1–Ni1–N2 97.3(2)°, N1–Ni1–S1 102.1(1)°, N2–Ni1–S2 102.9(1)°, O1–S1–S2 107.4(2)°, O2–S2–S1 107.4(2)°.

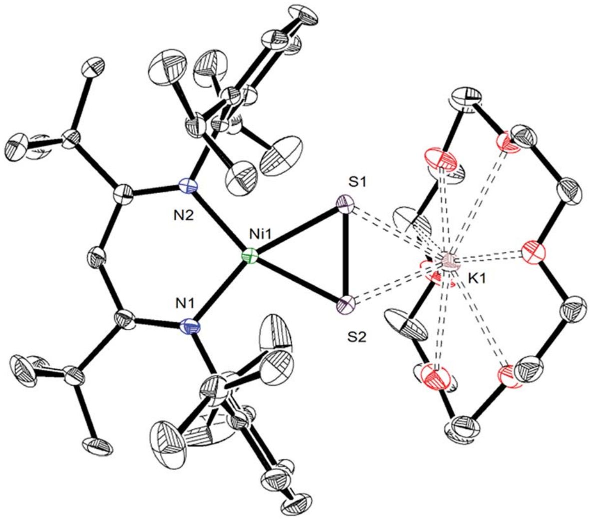

Fig. 3 ORTEP drawing of [K(18-crown-6)][$L^{tBu}Ni^{II}(\eta^2\text{-}S_2)$]·$2C_7H_8$ (**3**·$2C_7H_8$) shown with 50% thermal ellipsoids. Hydrogen atoms and C_7H_8 solvate molecules have been omitted for clarity. Selected metrical parameters: S1–S2 2.050(2) Å, Ni1–S1 2.202(2) Å, Ni1–S2 2.199(2) Å, Ni1–N1 1.900(4) Å, Ni1–N2 1.906(4) Å, S1–K1 3.248(2) Å, S2–K1 3.249(2) Å, N1–Ni1–N2 98.0(2)°, N1–Ni1–S2 103.1(1)°, N2–Ni1–S1 103.4(1)°.

Synthesis of an $[\eta^2\text{-}S_2]^{2-}$ complex

To further support the formation of the disulfide ($[\eta^2\text{-}S_2]^{2-}$) complex, [K(18-crown-6)][$L^{tBu}Ni^{II}(\eta^2\text{-}S_2)$] (**3**), during the synthesis of **1**, we endeavored to independently synthesize **3**. We, and others, have previously shown that terminal metal sulfides can react with S_8 to form metal disulfides.[39–41] Thus, we explored the reaction of [K(18-crown-6)][$L^{tBu}Ni^{II}(S)$] (**I**) with elemental sulfur. Addition of 0.125 equiv. of S_8 to a toluene solution of [K(18-crown-6)][$L^{tBu}Ni^{II}(S)$] results in a rapid color change from brown to orange. Work-up of the reaction mixture affords [K(18-crown-6)][$L^{tBu}Ni^{II}(\eta^2\text{-}S_2)$] (**3**), as an orange crystalline solid in 81% yield (eqn (3)). The solid state molecular structure of **3** is shown in Fig. 3. The disulfide (S_2^{2-}) ligand in **3** has a S–S distance of 2.050(2) Å, consistent with a single bond.[18] This distance is comparable to those reported for other $Ni^{II}(\eta^2\text{-}S_2)$ complexes.[42–49] The Ni–S distances (2.202(2) and 2.199(2) Å) in **3** are consistent with single bonds, and are much longer than the Ni–S bond length in the starting material (**I**, 2.064(2) Å). Finally, the Ni–N bonds in **3** are similar to those found in other square planar Ni^{II} β-diketiminate complexes.[16,49,50]

The ^1H NMR spectrum of **3** in toluene-d_8 (Fig. S7†) is consistent with a C_{2v} symmetric, diamagnetic, square planar Ni^{II} complex and features one *tert*-butyl resonance at 1.30 ppm and a single γ-CH resonance at 5.46 ppm. Importantly, this latter resonance is also present in the *in situ* ^1H NMR spectrum of the thermolysis of **II** (Fig. S3†), confirming the formation of **3** during that reaction, *via* an as-yet-unknown mechanism.

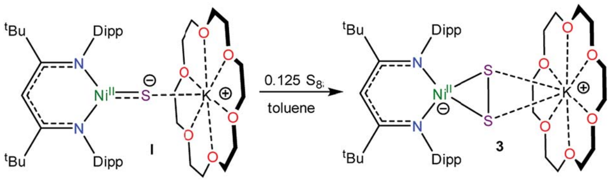

(3)

Reactivity of the $[\eta^2\text{-SO}]^{2-}$ ligand

While the reactivity of the SO ligand has not been well established, it is known to react with phosphines. For example, Schmid and co-workers reported that [$(\text{diphos})_2Ir(\eta^2\text{-OSSO})$][Cl] reacted with PPh_3 to form Ph_3PO, Ph_3PS, and [$(\text{diphos})_2IrCl$].[36] Similarly, Rauchfuss and co-workers demonstrated that $Cp_2Nb(S_2O)Cl$ reacted with Ph_3P to form $Cp_2Nb(O)Cl$ and two equiv. of Ph_3PS.[29] Both transformations were presumed to proceed through an unobserved SO intermediate. More recently, Mizobe *et al.* reported that PPh_3 could abstract an O-atom from the

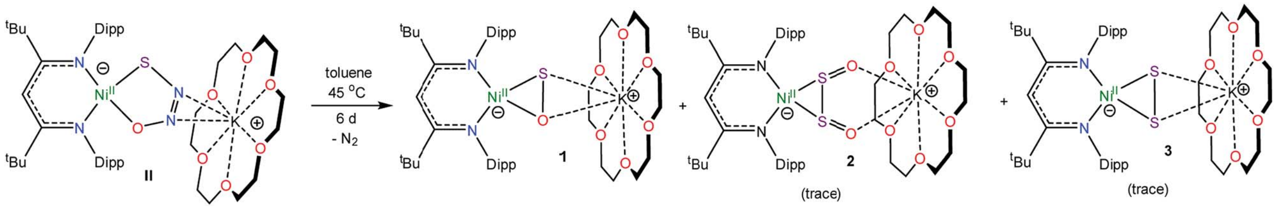

(2)

thioperoxide ligand in [(Cp′RuCl)$_2$(SbCl$_2$)(μ-Cl)(μ$_3$:κ^2-SO)] (Cp′ = C$_5$Me$_4$Et).[25] In contrast, the reactivity of the SO ligand with CO has not been studied. Accordingly, we explored the reactivity of [K(18-crown-6)][L$^{t\mathrm{Bu}}$Ni$^{\mathrm{II}}$(η^2-SO)] (**1**) with this substrate. Thus, exposure of a C$_6$D$_6$ solution of complex **1** to an atmosphere of ^{13}CO results in complete consumption of **1** after 6 h. A ^{13}C{^{1}H} NMR spectrum (Fig. S11†) of the reaction mixture reveals the formation of several ^{13}C-enriched products, indicating the incorporation of ^{13}CO. Specifically, this spectrum features resonances at 214.7, 177.3, 165.3, and 152.9 ppm, which are assignable to [K(18-crown-6)][L$^{t\mathrm{Bu}}$Ni$^{\mathrm{II}}$(η^2-SCO)] (**4**),[51] [K(18-crown-6)][L$^{t\mathrm{Bu}}$Ni$^{\mathrm{II}}$(*S*,*O*:κ^2-SCO$_2$)] (**5**), [K(18-crown-6)][L$^{t\mathrm{Bu}}$Ni(κ^2-CO$_3$)] (**6**), and SCO (**7**),[52] respectively (Scheme 1). This spectrum also features a minor ^{13}C-enriched resonance at 206.9 ppm, which we have tentatively assigned to [K(18-crown-6)][L$^{t\mathrm{Bu}}$Ni$^{\mathrm{II}}$(S$_2$CO)] (**8**), on the basis of the similarity of its dithiocarbonate ([S$_2$CO]$^{2-}$) chemical shift with those reported for other dithiocarbonate complexes.[52–54]

A ^{1}H NMR spectrum of the reaction mixture further supports these assignments. Specifically, an examination of the γ-CH region of this spectrum reveals overlapping resonances at 5.48 ppm (Fig. S10†), which are assignable to [K(18-crown-6)][L$^{t\mathrm{Bu}}$Ni$^{\mathrm{II}}$(η^2-SCO)] (**4**)[51] and [K(18-crown-6)][L$^{t\mathrm{Bu}}$Ni$^{\mathrm{II}}$(*S*,*O*:κ^2-SCO$_2$)] (**5**), and a resonance at 5.42 ppm, assignable to [K(18-crown-6)][L$^{t\mathrm{Bu}}$Ni(κ^2-CO$_3$)] (**6**). This spectrum also contains a minor resonance at 5.57 ppm that has been tentatively assigned to [K(18-crown-6)][L$^{t\mathrm{Bu}}$Ni$^{\mathrm{II}}$(S$_2$CO)] (**8**). Interestingly, at short reaction times, we observe the presence of a paramagnetic intermediate in the reaction mixture (Fig. S9†). We have identified this intermediate as the Ni$^{\mathrm{II}}$ sulfide, [K(18-crown-6)][L$^{t\mathrm{Bu}}$Ni$^{\mathrm{II}}$(S)] (**I**), on the basis of the similarity of its ^{1}H NMR resonances with those of the previously characterized material.[16] For example, this intermediate features diagnostic resonances at −130.25, −0.63, and 5.87 ppm, which are assignable to the γ-proton of the L$^{t\mathrm{Bu}}$ ligand, its ^{t}Bu substituents, and one environment of its diastereotopic ^{i}Pr methyl groups, respectively. For comparison, these resonances appear at −115.21, −0.88, and 6.56 ppm, respectively, for authentic **I**.[16] This intermediate is quickly formed upon addition of ^{13}CO, but its signals immediately begin to decay, and they are completely absent after 6 h (Fig. S9†).

We also characterized the products of the reaction of **1** and CO by IR spectroscopy. An IR spectrum of the reaction residue, dissolved in hexanes, reveals the presence of ν_{CO} modes at 2021, 1666, and 1620 cm^{-1} (Fig. S24†), which are assignable to the ν_{CO} modes of [L$^{t\mathrm{Bu}}$Ni$^{\mathrm{I}}$(CO)] (**9**),[55] [K(18-crown-6)][L$^{t\mathrm{Bu}}$Ni$^{\mathrm{II}}$(η^2-SCO)] (**4**),[51] and [K(18-crown-6)][L$^{t\mathrm{Bu}}$Ni$^{\mathrm{II}}$(κ^2-CO$_3$)] (**6**), respectively. Curiously, though, we do not observe any signals in the ^{1}H NMR spectrum of the reaction mixture that could be assigned to paramagnetic **9**, suggesting that it is only a minor product of the reaction.

The ^{13}C NMR spectrum of the *in situ* reaction mixture also features a minor ^{13}C-enriched resonance at 178.5, as well as a major resonance at 191.4 ppm (Fig. S11†). While these two resonances remain unassigned, we know that neither of the peaks is assignable to [K(18-crown-6)][L$^{t\mathrm{Bu}}$Ni$^{\mathrm{II}}$(η^2-CO$_2$)] (**10**), as we have performed the independent synthesis of this complex for spectroscopic comparison (see below). We also do not observe a resonance that could be assignable to free CO$_2$.

Finally, we observe no reaction between [K(18-crown-6)][L$^{t\mathrm{Bu}}$Ni$^{\mathrm{II}}$(η^2-SO)] (**1**) and PPh$_3$ in C$_6$D$_6$, according to ^{1}H and ^{31}P NMR spectroscopies. The lack of reactivity of the [SO]$^{2-}$ ligand in **1** with PPh$_3$ is somewhat surprising on the basis of thermodynamic considerations,[56] and could reflect steric shielding of the [SO]$^{2-}$ ligand by the bulky Dipp substituents.

Synthesis of an [*S*,*O*:κ^2-SCO$_2$]$^{2-}$ complex

To further support the formation of [K(18-crown-6)][L$^{t\mathrm{Bu}}$Ni$^{\mathrm{II}}$(*S*,*O*:κ^2-SCO$_2$)] (**5**) upon reaction of **1** with CO, we pursued its synthesis *via* an independent route. Thus, exposure of a C$_6$D$_6$ solution of [K(18-crown-6)][L$^{t\mathrm{Bu}}$Ni$^{\mathrm{II}}$(S)] (**I**) to excess carbon dioxide (CO$_2$) results in a rapid color change from deep brown to gold. The ^{1}H NMR spectrum of the reaction mixture taken 15 min after addition of CO$_2$ reveals full consumption of the starting material and formation of a new diamagnetic product whose spectroscopic signatures are consistent with a square planar Ni$^{\mathrm{II}}$ complex.[51] Work-up of the reaction mixture provides **5** as a pale brown crystalline solid in 57% yield (eqn (4)). The solid state molecular structure of **5** is shown in Fig. 4. The thiocarbonate ([*S*,*O*:κ^2-SCO$_2$]$^{2-}$) ligand in **5** features a μ:κ^2,κ^2 binding mode and is disordered over two positions, which are related by a C_2 rotation about the Ni–K vector, in a 87 : 13 ratio. The S–C (1.756(4) Å) and O–C (1.279(5) and 1.238(4) Å) bond lengths in **5** are consistent with those observed for previously reported [SCO$_2$]$^{2-}$ complexes,[57,58] while the Ni–S and Ni–O distances are 2.234(1) Å and 1.922(3) Å, respectively. Moreover, the K–S and K–O distances are 3.531(1) Å and 2.715(3) Å, respectively, which are comparable to other K–S and K–O dative interactions.[59,60] Finally, the Ni–N distances in **5** are comparable to those found in the starting material.[16] To the best of our

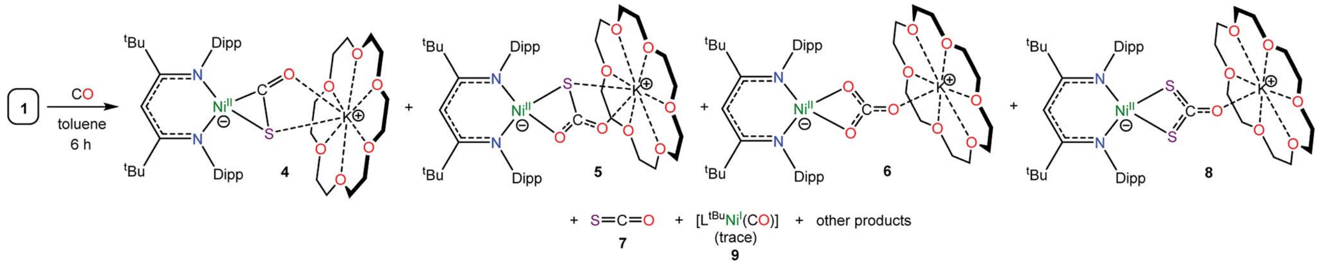

Scheme 1

knowledge, complex **5** is the first structurally characterized transition metal complex containing the $[SCO_2]^{2-}$ ligand. Other structurally characterized thiocarbonate complexes include $[\{((^{Ad}ArO)_3N)U\}_2(\mu\text{-}\eta^1,(O){:}\kappa^2(O',S)SCO_2)]$, prepared by reaction of $[\{((^{Ad}ArO)_3N)U\}_2(\mu\text{-}S)]$ with CO_2, and $[Cp^*{}_2Sm(\mu\text{-}\eta^1{:}\kappa^2\text{-}SCO_2)SmCp^*{}_2]$, prepared *via* reaction of $[(Cp^*{}_2Sm)_2(\mu\text{-}O)]$ with COS.[57,58]

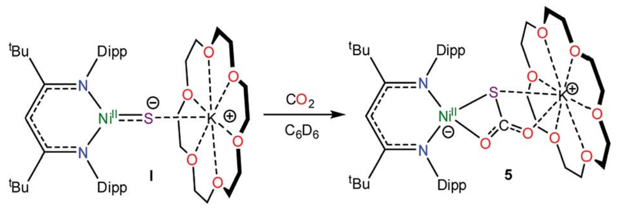

(4)

The $^{13}C\{^1H\}$ NMR spectrum of **5** in benzene-d_6 features a resonance at 177.3 ppm, which we have assigned to the $[S,O{:}\kappa^2\text{-}SCO_2]^{2-}$ moiety (Fig. S13†). This chemical shift is identical to the resonance assigned to this complex in the *in situ* ^{13}C NMR spectrum of the reaction of **1** with CO (Fig. S11†). Moreover, the ^1H NMR spectrum of **5** in C_6D_6 features a γ-CH resonance at 5.48 ppm. This resonance is also present in the *in situ* ^1H NMR spectrum of the reaction mixture of **1** and ^{13}CO (Fig. S10†), further confirming its formation in that transformation. Overall, these data conclusively demonstrate that complex **5** is formed during reduction of $[K(18\text{-crown-}6)][L^{tBu}Ni^{II}(\eta^2\text{-}SO)]$ (**1**) with CO.

Synthesis of an $[\kappa^2\text{-}CO_3]^{2-}$ complex

To further support the formation of $[K(18\text{-crown-}6)][L^{tBu}Ni(\kappa^2\text{-}CO_3)]$ (**6**) upon reaction of **1** with CO, we pursued its synthesis *via* an independent route. The hexameric nickel carbonate complex, $[K]_6[L^{tBu}Ni^{II}(\kappa^2\text{-}CO_3)]_6$,[11] first reported by Limberg and coworkers in 2012, was found to serve as a convenient starting material for the synthesis of $[K(18\text{-crown-}6)][L^{tBu}Ni^{II}(\kappa^2\text{-}CO_3)]$ (**6**). Addition of 6 equiv. of 18-crown-6 to a suspension of $[K]_6[L^{tBu}Ni^{II}(\kappa^2\text{-}CO_3)]_6$ results in the formation of complex **6** in 52% yield (eqn (5)). Its solid state molecular structure is shown in Fig. 5. The carbonate $(CO_3{}^{2-})$ ligand in **6** features a $\mu{:}\kappa^2,\eta^1$ binding mode, identical to that observed for the trithiocarbonate $(CS_3{}^{2-})$ ligand in $[K(18\text{-crown-}6)][L^{tBu}Ni(\kappa^2\text{-}CS_3)]$.[50] The O1–C1 (1.306(7) Å), O2–C1 (1.309(7) Å), and O3–C1 (1.242(7) Å) bond lengths in **6** are consistent with those reported for $[K]_6[L^{tBu}Ni^{II}(\kappa^2\text{-}CO_3)]_6$,[11] while the Ni–O1 and Ni–O2 distances are 1.882(4) and 1.901(4) Å, respectively, which are similar to those reported for the starting material.

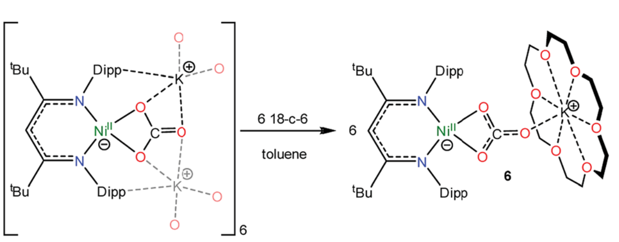

(5)

The $^{13}C\{^1H\}$ NMR spectrum of **6** in C_6D_6 features a resonance at 165.3 ppm, which is assignable to the $[CO_3]^{2-}$ moiety (Fig. S15†). This chemical shift matches the resonance assigned to this complex in the *in situ* ^{13}C NMR spectrum of the reaction mixture of **1** and ^{13}CO (Fig. S11†). In addition, the ^1H NMR spectrum of **6** in C_6D_6 features a γ-CH resonance at 5.42 ppm,

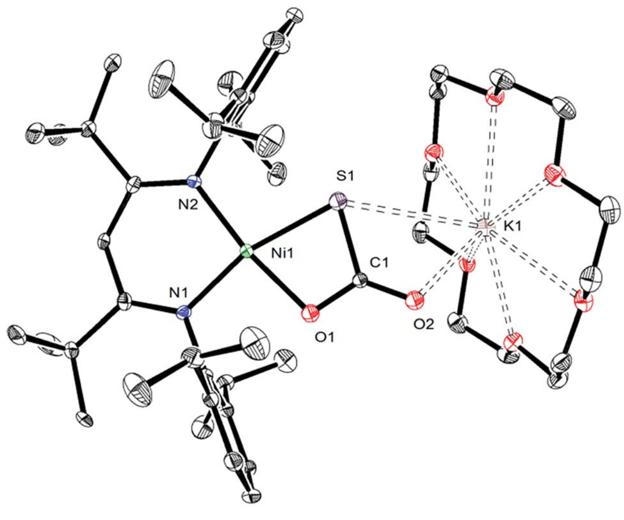

Fig. 4 ORTEP drawing of $[K(18\text{-crown-}6)][L^{tBu}Ni^{II}(S,O{:}\kappa^2\text{-}SCO_2)]\cdot1.5C_7H_8$ ($\mathbf{5}\cdot1.5C_7H_8$) shown with 50% thermal ellipsoids. Hydrogen atoms, C_7H_8 solvate molecules, and one orientation of the disordered $[S,O{:}\kappa^2\text{-}SCO_2]^{2-}$ ligand have been omitted for clarity. Selected metrical parameters: S1–C1 1.756(4) Å, O1–C1 1.279(5) Å, O2–C1 1.238(4) Å, Ni1–S1 2.234(1) Å, Ni1–O1 1.922(3) Å, Ni1–N1 1.904(3) Å, Ni1–N2 1.899(3) Å, S1–K1 3.531(1) Å, O2–K1 2.715(3) Å, S1–C1–O1 108.0(3)°, S1–C1–O2 126.2(3)°, O1–C1–O2 125.9(4)°, N1–Ni1–N2 96.7(1)°, N1–Ni1–O1 91.5(1)°, N2–Ni1–S1 99.22(9)°.

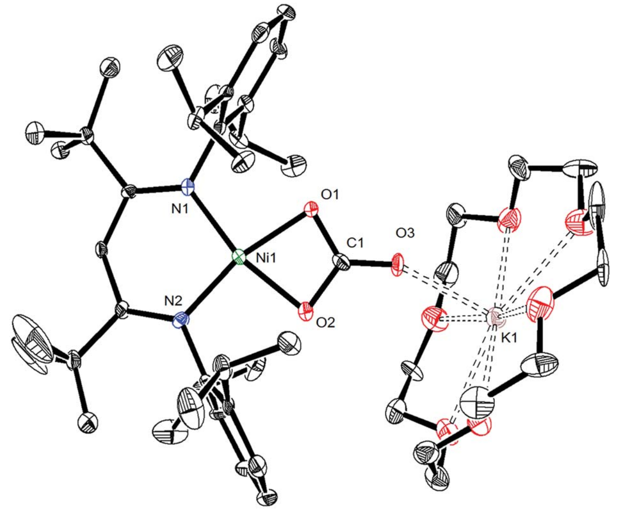

Fig. 5 ORTEP drawing of $[K(18\text{-crown-}6)][L^{tBu}Ni^{II}(\kappa^2\text{-}CO_3)]\cdot0.5C_5H_{12}$ ($\mathbf{6}\cdot0.5C_5H_{12}$) shown with 50% thermal ellipsoids. Hydrogen atoms, a C_5H_{12} solvate molecule, and a second independent molecule of $[K(18\text{-crown-}6)][L^{tBu}Ni^{II}(\kappa^2\text{-}CO_3)]$ have been omitted for clarity. Selected metrical parameters: C1–O1 1.306(7) Å, C1–O2 1.309(7) Å, C1–O3 1.242(7) Å, Ni1–O1 1.882(4) Å, Ni1–O2 1.901(4) Å, Ni1–N1 1.883(5) Å, Ni1–N2 1.879(5) Å, O3–K1 2.510(4) Å, O1–C1–O2 110.8(5)°, O1–C1–O3 125.0(6)°, N1–Ni1–N2 97.9(2)°, N1–Ni1–O1 96.6(2)°, N2–Ni1–O2 96.5(2)°.

which is present in the *in situ* ^{1}H NMR spectrum of the reaction mixture of **1** and ^{13}CO (Fig. S10†). The IR spectrum (hexanes solution) of **6** features a strong ν_{CO} mode at 1620 cm^{-1}, which is also present in a solution IR spectrum of the reaction mixture formed upon addition of CO to **1** (Fig. S24†). Overall, these data conclusively demonstrate that complex **6** is formed during reduction of $[\mathrm{K(18\text{-}crown\text{-}6)}][\mathrm{L}^{t\mathrm{Bu}}\mathrm{Ni}^{\mathrm{II}}(\eta^2\text{-SO})]$ (**1**) with CO.

Synthesis of an $[\eta^2\text{-CO}_2]^{2-}$ complex

In an effort to assign the resonance at 191.4 ppm in the *in situ* ^{13}C{^{1}H} NMR spectrum of the reaction of **1** and ^{13}CO, we endeavored to independently synthesize the carbon dioxide complex, $[\mathrm{K(18\text{-}crown\text{-}6)}][\mathrm{L}^{t\mathrm{Bu}}\mathrm{Ni}^{\mathrm{II}}(\eta^2\text{-CO}_2)]$ (**10**). We rationalized that **10** was a plausible reaction product, given the formation of CO_2 during the reaction (see below). Several previously reported $Ni(CO_2)$ complexes have been synthesized by reaction of CO_2 with a Ni^0 precursor.[61–64] In a similar vein, the Ni(0)–N$_2$ complex, $[\mathrm{K}]_2[\mathrm{L}^{t\mathrm{Bu}}\mathrm{Ni}^0(\mu\text{-}\eta^1\text{:}\eta^1\text{-N}_2)\mathrm{Ni}^0\mathrm{L}^{t\mathrm{Bu}}]$, previously reported by Limberg and co-workers in 2009,[65] was found to serve as an effective Ni^0 source for the synthesis of **10**. Thus, exposure of $[\mathrm{K}]_2[\mathrm{L}^{t\mathrm{Bu}}\mathrm{Ni}^0(\mu\text{-}\eta^1\text{:}\eta^1\text{-N}_2)\mathrm{Ni}^0\mathrm{L}^{t\mathrm{Bu}}]$ to two equiv. of CO_2, followed by addition of 18-crown-6, resulted in the formation of **10** (eqn (6)), which was isolated as pale orange plates in 41% yield after work-up. Its formulation was confirmed by X-ray crystallography and its solid state molecular structure is shown in Fig. 6.

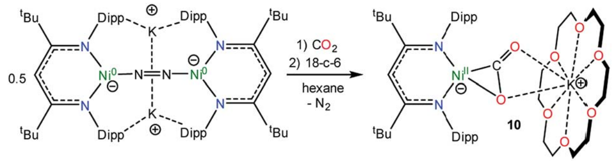

(6)

Complex **10** features a square planar Ni$^{\mathrm{II}}$ center ligated by the β-diketiminate ligand and a $[CO_2]^{2-}$ ligand. The $[CO_2]^{2-}$ ligand in **10** features a $\mu\text{:}\eta^2,\kappa^2$ binding mode, similar to that observed for the $[COS]^{2-}$ ligand in complex **4**. The $[CO_2]^{2-}$ ligand in **10** is disordered over two positions, in a 76 : 24 ratio, which are related by a C_2 rotation axis about the Ni–K vector. The Ni1–O1 (1.897(6) Å) and Ni1–C1 (1.890(6) Å) distances are consistent with those previously reported for the $\mathrm{Ni}(\eta^2\text{-CO}_2)$ fragment.[61,62,64,66,67] Additionally, the Ni–N bonds in **10** are consistent with those found in other square planar Ni$^{\mathrm{II}}$ β-diketiminate complexes.[16,49,50]

The ^{1}H NMR spectrum of **10** in C_6D_6 is consistent with that expected for a C_s symmetric, square planar Ni$^{\mathrm{II}}$ complex. It features two *tert*-butyl resonances at 1.42 and 1.34 ppm, and a single γ-CH resonance at 5.42 ppm. Its ^{13}C{^{1}H} NMR spectrum in C_6D_6 features a resonance at 167.2 ppm, which we have assigned to the $[\eta^2\text{-CO}_2]^{2-}$ ligand. This chemical shift is consistent with those reported for previously isolated $\mathrm{Ni}(\eta^2\text{-CO}_2)$ complexes.[62–64] Most importantly, however, these resonances are not observed in the *in situ* ^{13}C{^{1}H} and ^{1}H NMR spectra of the reaction between **1** and ^{13}CO (Fig. S10 and 11†). Thus, we can definitively conclude that complex **10** is not being formed in that reaction. Finally, complex **10** features a ν_{CO} mode at 1664 cm^{-1} in its IR spectrum (KBr pellet), which is similar to those reported for other nickel CO_2 complexes.[62–64] This vibration is also not present in the *in situ* IR spectrum (recorded in hexanes) of the reaction residue formed upon reaction of **1** with CO (Fig. S24†).

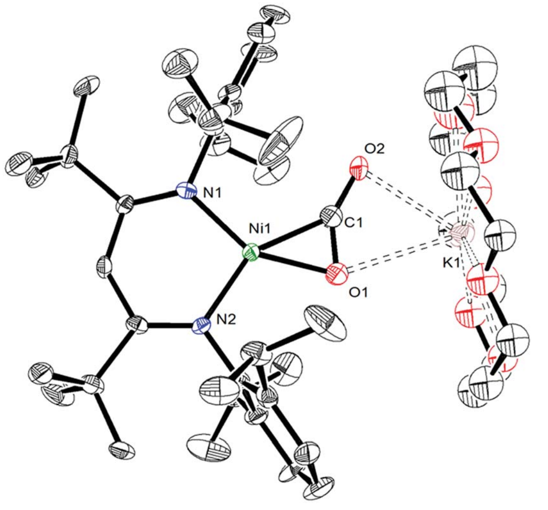

Fig. 6 ORTEP drawing of $[\mathrm{K(18\text{-}crown\text{-}6)}][\mathrm{L}^{t\mathrm{Bu}}\mathrm{Ni}^{\mathrm{II}}(\eta^2\text{-CO}_2)]\cdot 2C_6H_6$ ($\mathbf{10}\cdot 2C_6H_6$) shown with 50% thermal ellipsoids. Hydrogen atoms, C_6H_6 solvate molecules, and second orientations of the CO_2 and 18-crown-6 fragments have been omitted for clarity. Selected metrical parameters: C1–O1 1.231(9) Å, C1–O2 1.22(1) Å, Ni1–C1 1.890(6) Å, Ni1–O1 1.897(6) Å, Ni1–N1 1.901(6) Å, Ni1–N2 1.896(5) Å, O1–K1 2.980(6) Å, O2–K1 2.71(1) Å, O1–C1–O2 144.0(8)°, N1–Ni1–N2 99.2(2)°, N1–Ni1–C1 112.2(3)°, N2–Ni1–O1 110.7(3)°.

Mechanistic considerations

To rationalize the formation of complexes **4** and **5**, we propose that CO initially reacts with **1** to form CO_2 and $[\mathrm{K(18\text{-}crown\text{-}6)}][\mathrm{L}^{t\mathrm{Bu}}\mathrm{Ni}^{\mathrm{II}}(\mathrm{S})]$ (**I**) (Scheme 2). Complex **I** then reacts with either CO or CO_2 to yield $[\mathrm{K(18\text{-}crown\text{-}6)}][\mathrm{L}^{t\mathrm{Bu}}\mathrm{Ni}^{\mathrm{II}}(\eta^2\text{-SCO})]$ (**4**) or $[\mathrm{K(18\text{-}crown\text{-}6)}][\mathrm{L}^{t\mathrm{Bu}}\mathrm{Ni}^{\mathrm{II}}(S,O\text{:}\kappa^2\text{-SCO}_2)]$ (**5**), respectively. Significantly, their presence, along with the observation of $[\mathrm{K(18\text{-}crown\text{-}6)}][\mathrm{L}^{t\mathrm{Bu}}\mathrm{Ni}^{\mathrm{II}}(\mathrm{S})]$ (**I**) in the reaction mixture, demonstrates the formal reduction of N_2O by CO, as originally envisioned. That said, the reaction rates of **I** with CO and CO_2 are qualitatively similar to the reaction rate of **I** with N_2O. As a consequence, **I** is unlikely to be an effective catalyst for N_2O reduction because off-cycle reactions with CO and CO_2 would be competitive with the desired N_2O capture reaction (Scheme 2).

To rationalize the formation of complex **6** and COS, we propose that reaction of the newly formed CO_2 with unreacted **1** results in the formation of a transient, unobserved nickel monothiopercarbonate complex, $[\mathrm{K(18\text{-}crown\text{-}6)}][\mathrm{L}^{t\mathrm{Bu}}\mathrm{Ni}^{\mathrm{II}}(\kappa^2\text{-SOCO}_2)]$ (**11**). Complex **11** then transfers a sulfur atom to CO to form $[\mathrm{K(18\text{-}crown\text{-}6)}][\mathrm{L}^{t\mathrm{Bu}}\mathrm{Ni}^{\mathrm{II}}(\kappa^2\text{-CO}_3)]$ (**6**) and COS (**7**) (Scheme 2), both of which were confirmed to be present in the *in situ* reaction mixture. This hypothesis also nicely explains the presence of $[\mathrm{K(18\text{-}crown\text{-}6)}][\mathrm{L}^{t\mathrm{Bu}}\mathrm{Ni}^{\mathrm{II}}(\kappa^2\text{-S}_2\mathrm{CO})]$ (**8**), which could be formed *via* the reaction of **7** with **I** (Scheme 2). While a monothiopercarbonate complex has not been previously reported, the reaction of metal peroxides (O_2^{2-}) with CO_2 is

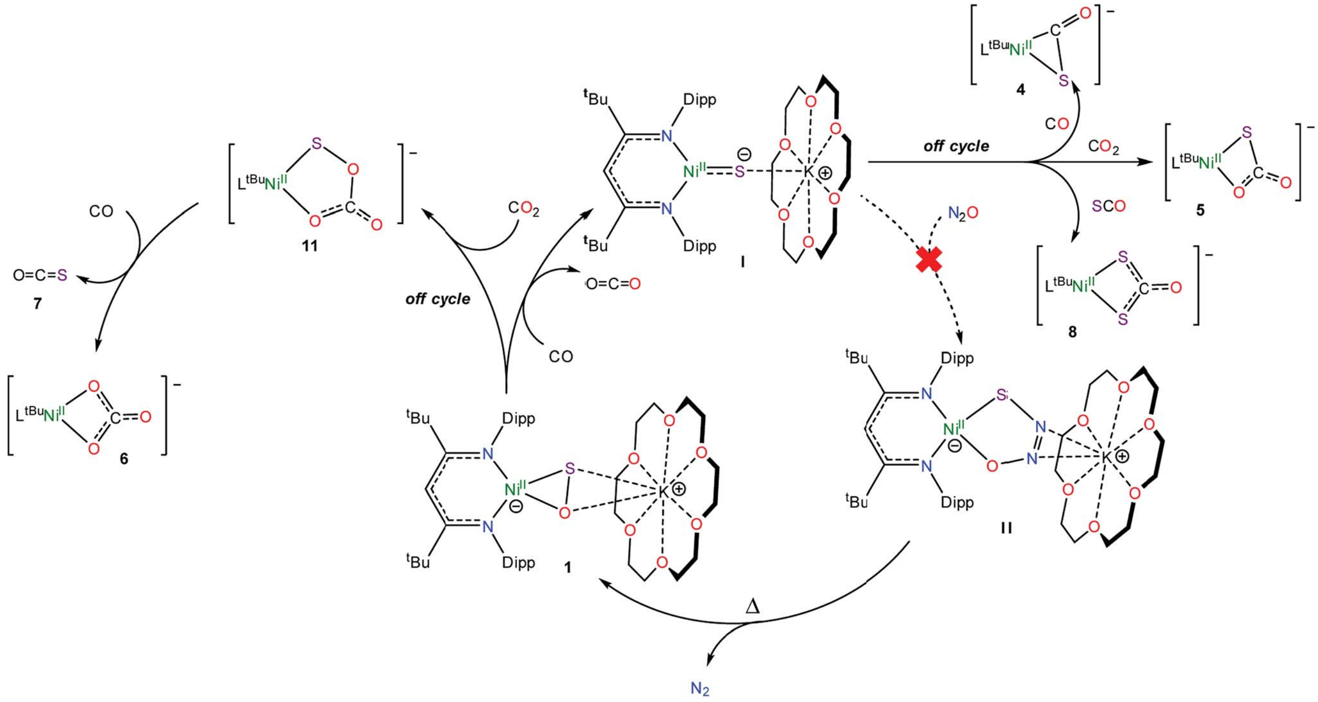

Scheme 2

known to yield peroxocarbonate ([OOCO$_2$]$^{2-}$) complexes.[68–71] Similarly, metal disulfides (S$_2$$^{2-}$) are known to react with CS$_2$ to form perthiocarbonates ([SSCS$_2$]$^{2-}$).[72,73] Moreover, peroxocarbonates are known to be very effective O-atom donors.[69,74–77]

Consistent with this hypothesis, reaction of [K(18-crown-6)][$L^{tBu}Ni^{II}(\eta^2$-SO)] (**1**) with CO$_2$ in C$_6$D$_6$ results in the rapid formation of a new diamagnetic Ni^{II} complex, as evidenced by the appearance of diagnostic resonances at 4.49 ppm (γ-CH) and 1.20 ppm (*t*Bu) in the *in situ* ^{1}H NMR spectrum of the reaction mixture (Fig. S18†). We have assigned these resonances to the monothiopercarbonate complex [K(18-crown-6)][$L^{tBu}Ni^{II}(\kappa^2$-SOCO$_2$)] (**11**) (eqn (7)). Complex **11** is the only product observed in the reaction mixture. These results provide further support for the overall reaction mechanism proposed in Scheme 2 and suggest that (SOCO$_2$)$^{2-}$ could function as a very effective a S-atom transfer reagent.[78]

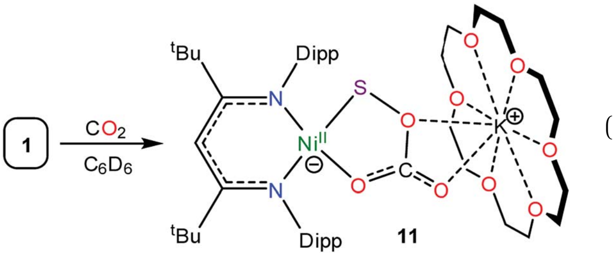

(7)

Conclusions

Gentle thermolysis of the thiohyponitrite complex, [K(18-crown-6)][$L^{tBu}Ni^{II}(\kappa^2$-SNNO)], results in extrusion of N$_2$ and formation of [K(18-crown-6)][$L^{tBu}Ni^{II}(\eta^2$-SO)], a rare example of a structurally characterized SO complex, along with trace amounts of [K(18-crown-6)][$L^{tBu}Ni^{II}(\eta^2$-OSSO)] and [K(18-crown-6)][$L^{tBu}Ni^{II}(\eta^2$-S$_2$)]. [K(18-crown-6)][$L^{tBu}Ni^{II}(\eta^2$-SO)] reacts rapidly with CO, forming the "masked" terminal Ni(II) sulfide intermediate, [K(18-crown-6)][$L^{tBu}Ni^{II}$(S)], along with CO$_2$, *via* O-atom abstraction. This Ni(II) sulfide intermediate then reacts with CO or CO$_2$ to form [K(18-crown-6)][$L^{tBu}Ni^{II}(\eta^2$-SCO)] and [K(18-crown-6)][L^{tBu}Ni(*S*,*O*:κ^2-SCO$_2$)], respectively. [K(18-crown-6)][$L^{tBu}Ni^{II}(\eta^2$-SO)] can also react with the newly formed CO$_2$ to form a putative monothiopercarbonate complex, [K(18-crown-6)][$L^{tBu}Ni^{II}(\kappa^2$-SOCO$_2$)], which can then transfer an S atom to CO, forming COS and [K(18-crown-6)][$L^{tBu}Ni^{II}(\kappa^2$-CO$_3$)].

Significantly, the observation of [K(18-crown-6)][$L^{tBu}Ni^{II}$(S)] in the reaction mixture, along with the formation of [K(18-crown-6)][$L^{tBu}Ni^{II}(\eta^2$-SCO)] and [K(18-crown-6)][$L^{tBu}Ni^{II}$(*S*,*O*:κ^2-SCO$_2$)], confirms that the SO ligand is susceptible to O-atom abstraction by CO, which had not been previously demonstrated. More importantly, these reaction products reveal the stepwise conversion of [K(18-crown-6)][$L^{tBu}Ni^{II}(\kappa^2$-SNNO)] to [K(18-crown-6)][$L^{tBu}Ni^{II}(\eta^2$-SO)] and then [K(18-crown-6)][$L^{tBu}Ni^{II}$(S)], which represents a formal reduction of N$_2$O by CO, forming N$_2$ and CO$_2$. Significantly, this transformation parallels the chemistry mediated by nano-particulate Pt/Rh in catalytic converters. In contrast to the metal-centered redox of the catalytic converter example, however, the redox chemistry in our system occurs at the sulfide ligand, while the nickel center remains in the 2+ oxidation state at every step. The use of ligand-centered redox is an intriguing strategy for N$_2$O reduction and we suggest that the study of model systems, such as the one presented in this manuscript, could inspire the design of a new generation of homogeneous and heterogeneous N$_2$O reduction catalysts.

Conflicts of interest

The authors declare no competing financial interests.

Acknowledgements

We thank the National Science Foundation (CHE 1361654) for financial support of this work. We would also like to thank the Scott Group at UCSB for the use of their ^{13}CO. This research made use of the 400 MHz NMR Spectrometer in the Department of Chemistry and Biochemistry, an NIH SIG (1S10OD012077-01A1).

References

1 A. R. Ravishankara, J. S. Daniel and R. W. Portmann, *Science*, 2009, **326**, 123–125.
2 W. C. Trogler, *Coord. Chem. Rev.*, 1999, **187**, 303–327.
3 A. V. Leontev, O. g. A. Fomicheva, M. V. Proskurnina and N. S. Zefirov, *Russ. Chem. Rev.*, 2001, **70**, 91.
4 M. J. Prather, *Science*, 1998, **279**, 1339–1341.
5 E. A. Davidson and D. Kanter, *Environ. Res. Lett.*, 2014, **9**, 105012.
6 M. Konsolakis, *ACS Catal.*, 2015, **5**, 6397–6421.
7 B. Neuffer, N. Frank and M. Desai, Available and Emerging Technologies for Reducing Greenhouse Gas Emissions from the Nitric Acid Production Industry, *Report of the Office of Air and Radiation*, U.S. Environmental Protection Agency, Research Triangle Park, NC, 2010.
8 M. Dameris, *Angew. Chem., Int. Ed.*, 2010, **49**, 489–491.
9 P. Granger and V. I. Parvulescu, *Chem. Rev.*, 2011, **111**, 3155–3207.
10 J. P. Reeds, B. L. Yonke, P. Y. Zavalij and L. R. Sita, *J. Am. Chem. Soc.*, 2011, **133**, 18602–18605.
11 B. Horn, C. Limberg, C. Herwig, M. Feist and S. Mebs, *Chem. Commun.*, 2012, **48**, 8243–8245.
12 A. W. Kaplan and R. G. Bergman, *Organometallics*, 1998, **17**, 5072–5085.
13 J.-H. Lee, M. Pink, J. Tomaszewski, H. Fan and K. G. Caulton, *J. Am. Chem. Soc.*, 2007, **129**, 8706–8707.
14 L. E. Doyle, W. E. Piers and J. Borau-Garcia, *J. Am. Chem. Soc.*, 2015, **137**, 2187–2190.
15 R. Zeng, M. Feller, Y. Ben-David and D. Milstein, *J. Am. Chem. Soc.*, 2017, **139**, 5720–5723.
16 N. J. Hartmann, G. Wu and T. W. Hayton, *Angew. Chem., Int. Ed.*, 2015, **54**, 14956–14959.
17 K. Severin, *Chem. Soc. Rev.*, 2015, **44**, 6375–6386.
18 P. Pyykkö, *J. Phys. Chem. A*, 2015, **119**, 2326–2337.
19 F. X. Powell and D. R. Lide Jr, *J. Chem. Phys.*, 1964, **41**, 1413–1419.
20 B. Horn, C. Limberg, C. Herwig and B. Braun, *Inorg. Chem.*, 2014, **53**, 6867–6874.
21 C. Bianchini, C. Mealli, A. Meli and M. Sabat, *J. Chem. Soc., Chem. Commun.*, 1985, 1024–1025.
22 A. Neher, O. Heyke and I. P. Lorenz, *Z. Anorg. Allg. Chem.*, 1989, **578**, 185–190.
23 R. Huang, I. A. Guzei and J. H. Espenson, *Organometallics*, 1999, **18**, 5420–5422.
24 C. Minh Tuong, W. K. Hammons, A. L. Howarth, K. E. Lutz, A. D. Maduvu, L. B. Haysley, B. R. T. Allred, L. K. Hoyt, M. S. Mashuta and M. E. Noble, *Inorg. Chem.*, 2009, **48**, 5027–5038.
25 K. Oya, H. Seino, M. Akiizumi and Y. Mizobe, *Organometallics*, 2011, **30**, 2939–2946.
26 R. Wang, M. S. Mashuta, J. F. Richardson and M. E. Noble, *Inorg. Chem.*, 1996, **35**, 3022–3030.
27 L. E. Longobardi, V. Wolter and D. W. Stephan, *Angew. Chem., Int. Ed.*, 2015, **54**, 809–812.
28 L. Markó, B. Markó-Monostory, T. Madach and H. Vahrenkamp, *Angew. Chem., Int. Ed.*, 1980, **19**, 226–227.
29 J. E. Hoots, D. A. Lesch and T. B. Rauchfuss, *Inorg. Chem.*, 1984, **23**, 3130–3136.
30 S. Bagherzadeh and N. P. Mankad, *Chem. Commun.*, 2018, **54**, 1097–1100.
31 F. J. Lovas, E. Tiemann and D. R. Johnson, *J. Chem. Phys.*, 1974, **60**, 5005–5010.
32 R. D. Harcourt, *J. Mol. Struct.: THEOCHEM*, 1989, **186**, 131–165.
33 R. D. Harcourt, *Eur. J. Inorg. Chem.*, 2000, **2000**, 1901–1916.
34 M. A. Martin-Drumel, J. van Wijngaarden, O. Zingsheim, F. Lewen, M. E. Harding, S. Schlemmer and S. Thorwirth, *J. Mol. Spectrosc.*, 2015, **307**, 33–39.
35 C. J. Marsden and B. J. Smith, *Chem. Phys.*, 1990, **141**, 335–353.
36 G. Schmid, G. Ritter and T. Debaerdemaeker, *Chem. Ber.*, 1975, **108**, 3008–3013.
37 I.-P. Lorenz and J. Kull, *Angew. Chem., Int. Ed.*, 1986, **25**, 261–262.
38 The other structurally characterized example, $[(\text{diphos})_2\text{Ir(OSSO)}]\text{Cl}$ (diphos = $Ph_2PCH_2CH_2PPh_2$), features a *trans*-OSSO ligand (dihedral angle = 68°) with an S–S bond length of 2.041 Å. Curiously, one of its S–O bond lengths (1.21(2) Å) is anomalously short, which may indicate the presence of unresolved disorder in the structure. See ref. 36.
39 D. E. Smiles, G. Wu and T. W. Hayton, *Inorg. Chem.*, 2014, **53**, 12683–12685.
40 Z. K. Sweeney, J. L. Polse, R. A. Andersen, R. G. Bergman and M. G. Kubinec, *J. Am. Chem. Soc.*, 1997, **119**, 4543–4544.
41 Z. K. Sweeney, J. L. Polse, R. G. Bergman and R. A. Andersen, *Organometallics*, 1999, **18**, 5502–5510.
42 C. Mealli and S. Midollini, *Inorg. Chem.*, 1983, **22**, 2785–2786.
43 R. J. Pleus, H. Waden, W. Saak, D. Haase and S. Pohl, *J. Chem. Soc., Dalton Trans.*, 1999, 2601–2610.
44 J. Cho, K. M. Van Heuvelen, G. P. A. Yap, T. C. Brunold and C. G. Riordan, *Inorg. Chem.*, 2008, **47**, 3931–3933.
45 S. Yao, C. Milsmann, E. Bill, K. Wieghardt and M. Driess, *J. Am. Chem. Soc.*, 2008, **130**, 13536–13537.
46 M. Inosako, A. Kunishita, M. Kubo, T. Ogura, H. Sugimoto and S. Itoh, *Dalton Trans.*, 2009, 9410–9417.
47 V. M. Iluc, C. A. Laskowski, C. K. Brozek, N. D. Harrold and G. L. Hillhouse, *Inorg. Chem.*, 2010, **49**, 6817–6819.

48 F. Olechnowicz, G. L. Hillhouse and R. F. Jordan, *Inorg. Chem.*, 2015, **54**, 2705–2712.

49 S. Yao, Y. Xiong, X. Zhang, M. Schlangen, H. Schwarz, C. Milsmann and M. Driess, *Angew. Chem., Int. Ed.*, 2009, **48**, 4551–4554.

50 N. J. Hartmann, G. Wu and T. W. Hayton, *Dalton Trans.*, 2016, **45**, 14508–14510.

51 N. J. Hartmann, G. Wu and T. W. Hayton, *J. Am. Chem. Soc.*, 2016, **138**, 12352–12355.

52 W. S. Farrell, P. Y. Zavalij and L. R. Sita, *Angew. Chem., Int. Ed.*, 2015, **54**, 4269–4273.

53 J. D. E. T. Wilton-Ely, D. Solanki and G. Hogarth, *Inorg. Chem.*, 2006, **45**, 5210–5214.

54 R. Lalrempuia, A. Stasch and C. Jones, *Chem. Sci.*, 2013, **4**, 4383–4388.

55 B. Horn, S. Pfirrmann, C. Limberg, C. Herwig, B. Braun, S. Mebs and R. Metzinger, *Z. Anorg. Allg. Chem.*, 2011, **637**, 1169–1174.

56 R. H. Holm and J. P. Donahue, *Polyhedron*, 1993, **12**, 571–589.

57 O. P. Lam, S. M. Franke, F. W. Heinemann and K. Meyer, *J. Am. Chem. Soc.*, 2012, **134**, 16877–16881.

58 C. Schoo, S. V. Klementyeva, M. T. Gamer, S. N. Konchenko and P. W. Roesky, *Chem. Commun.*, 2016, **52**, 6654–6657.

59 D. E. Smiles, G. Wu and T. W. Hayton, *J. Am. Chem. Soc.*, 2014, **136**, 96–99.

60 D. E. Smiles, G. Wu, N. Kaltsoyannis and T. W. Hayton, *Chem. Sci.*, 2015, **6**, 3891–3899.

61 A. Döhring, P. W. Jolly, C. Krüger and M. J. Romão, *Z. Naturforsch. B Chem. Sci.*, 1985, **40**, 484–488.

62 R. Beck, M. Shoshani, J. Krasinkiewicz, J. A. Hatnean and S. A. Johnson, *Dalton Trans.*, 2013, **42**, 1461–1475.

63 Y.-E. Kim, J. Kim and Y. Lee, *Chem. Commun.*, 2014, **50**, 11458–11461.

64 J. S. Anderson, V. M. Iluc and G. L. Hillhouse, *Inorg. Chem.*, 2010, **49**, 10203–10207.

65 S. Pfirrmann, C. Limberg, C. Herwig, R. Stößer and B. Ziemer, *Angew. Chem., Int. Ed.*, 2009, **48**, 3357–3361.

66 C. H. Lee, D. S. Laitar, P. Mueller and J. P. Sadighi, *J. Am. Chem. Soc.*, 2007, **129**, 13802–13803.

67 D. Sahoo, C. Yoo and Y. Lee, *J. Am. Chem. Soc.*, 2018, **140**, 2179–2185.

68 P. Zimmermann, S. Hoof, B. Braun-Cula, C. Herwig and C. Limberg, *Angew. Chem., Int. Ed.*, 2018, **57**, 7230–7233.

69 K. Hashimoto, S. Nagatomo, S. Fujinami, H. Furutachi, S. Ogo, M. Suzuki, A. Uehara, Y. Maeda, Y. Watanabe and T. Kitagawa, *Angew. Chem., Int. Ed.*, 2002, **41**, 1202–1205.

70 G. Meier and T. Braun, *Angew. Chem., Int. Ed.*, 2012, **51**, 12564–12569.

71 M. Yamashita, K. Goto and T. Kawashima, *J. Am. Chem. Soc.*, 2005, **127**, 7294–7295.

72 D. Coucouvanis and M. Draganjac, *J. Am. Chem. Soc.*, 1982, **104**, 6820–6822.

73 S.-B. Yu and R. H. Holm, *Polyhedron*, 1993, **12**, 263–266.

74 A. McKillop and W. R. Sanderson, *Tetrahedron*, 1995, **51**, 6145–6166.

75 T. Tsugawa, H. Furutachi, M. Marunaka, T. Endo, K. Hashimoto, S. Fujinami, S. Akine, Y. Sakata, S. Nagatomo, T. Tosha, T. Nomura, T. Kitagawa, T. Ogura and M. Suzuki, *Chem. Lett.*, 2015, **44**, 330–332.

76 B. S. Lane, M. Vogt, V. J. DeRose and K. Burgess, *J. Am. Chem. Soc.*, 2002, **124**, 11946–11954.

77 H. Yao and D. E. Richardson, *J. Am. Chem. Soc.*, 2000, **122**, 3220–3221.

78 J. P. Donahue, *Chem. Rev.*, 2006, **106**, 4747–4783.